ELSEVIER

Polymer 42 (2001) 3859–3866

polymer

www.elsevier.nl/locate/polymer

Structure formation during the isothermal crystallization of oriented amorphous poly(ethylene terephthalate) films

J. Radhakrishnan[1], A. Kaito*

Department of Polymer Physics, National Institute of Materials and Chemical Research, Higashi, Tsukuba, Ibaraki, 305-8565 Japan

Received 5 April 2000; received in revised form 21 August 2000; accepted 22 September 2000

Abstract

Isothermal crystallization from the glassy state of oriented poly(ethylene terephthalate) (PET) was studied using in situ Fourier transform infrared (FTIR) spectroscopy, in situ wide-angle X-ray diffraction (WAXD) studies, and small angle X-ray scattering (SAXS) studies. The oriented amorphous films of PET were prepared by rolling melt-quenched films to a draw ratio of 2. In situ FTIR was used to investigate the ordering process of polymer chains prior to the crystallization by measuring the change in dichroic ratio with time while in situ WAXD was used to investigate the development of crystalline structure. The SAXS studies of the heat-treated PET showed that the density fluctuation was formed in the induction period. The density fluctuation is nearly isotropic in the early stage of the structural organization, but gradually orients to the stress direction until the onset of crystal growth. The long period decreases as crystallization proceeds, resulting in the formation of the regular long period of lamellar stacks. The structural organization during the isothermal crystallization of oriented PET consists of three stages. The first stage is the thermodynamic relaxation, occurring when the samples are heated above its T_g. The second stage is the self-organization process of the oriented amorphous structure, in which the degree of orientation increases with time from nearly isotropic state and the *gauche* conformation is transformed into the *trans* conformation. The crystalline reflections begin to appear in the third stage only after the orientation process is completed. These observations suggest that PET chains undergo ordering process in the induction period of crystallization.

Keywords: Crystallization; Poly(ethylene terephthalate); Conformation

1. Introduction

Recent studies on the crystallization of several polymers from the glassy state revealed the appearance of the transient mesophase before the actual crystallization process begins [1–8]. All these studies showed that parallel ordering of polymer chains takes place prior to crystallization. Imai et al. studied the crystallization of unoriented poly(ethylene terephthalate) (PET) from the glassy sate using small angle X-ray scattering (SAXS) and wide-angle X-ray diffraction (WAXD) studies. It was found that when the glassy PET was annealed at 115°C, a long-range ordered structure with a size of 20 nm is formed during the induction period of crystallization [1–4]. Long-range density fluctuation of the polymer chains has been suggested to be responsible for the ordering phenomena occurring during the induction period of crystallization [1–4]. It was suggested that the crystal nucleation occurs in the denser regions of the density fluctuation once the size of the fluctuation exceeds a given value [1–5].

Crystallization of PET in the oriented form also has attracted considerable attention owing to its use in the oriented form in most of the commercial applications [9–13]. Some of the earlier studies showed that the rate of crystallization is strongly dependent on the degree of orientation [9,10]. Asano et al. [11] studied the crystallization of oriented amorphous PET films by WAXD and microhardness measurements at temperatures ranging from 50 to 240°C. The WAXD studies revealed the appearance of smectic order at 60°C with a period of 1.07 nm followed by a layer structure at 70°C in the scale of 11 nm and finally a triclinic order was observed above 80°C. The appearance of the layer structure prior to the development of triclinic crystals was suggested to be associated with a density difference along the molecular direction produced by a molecular tilting mechanism. In situ studies on the crystallization of PET under strain and orientation using synchrotron radiation experiments showed some evidence of the formation of

* Corresponding author. Tel.: +81-298-61-6395; fax: +81-298-61-6232.
E-mail address: kaito@home.nimc.go.jp (A. Kaito).
[1] Present address: Procter & Gamble Far East Inc., Research & Development, 17 Koyo-cho Naka 1-chome, Higashinada-ku Kobe 658-0032 Japan.

0032-3861/01/$ - see front matter
PII: S0032-3861(00)00754-0

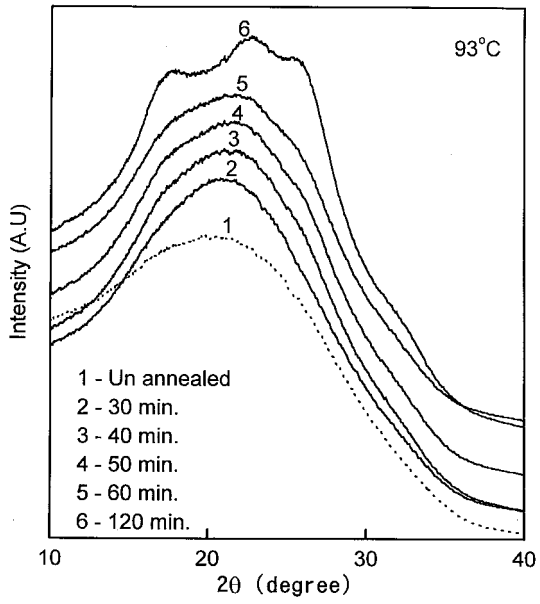

Fig. 1. WAXD intensity profiles at different time intervals for the samples with draw ratio (DR) = 2 during isothermal crystallization at 93°C.

oriented non-crystalline order prior to the beginning of the crystallization. It was also suggested that the oriented crystallization process is only limited by the local segmental mobility rather than the main chain mobility [12–15].

In the present work, the structure formation during the crystallization process of oriented amorphous PET film was studied using in situ Fourier transform infrared (FTIR) and in situ WAXD studies at temperatures close to the glass transition temperature. Changes in conformation and the orientation order of the polymer chains during the course

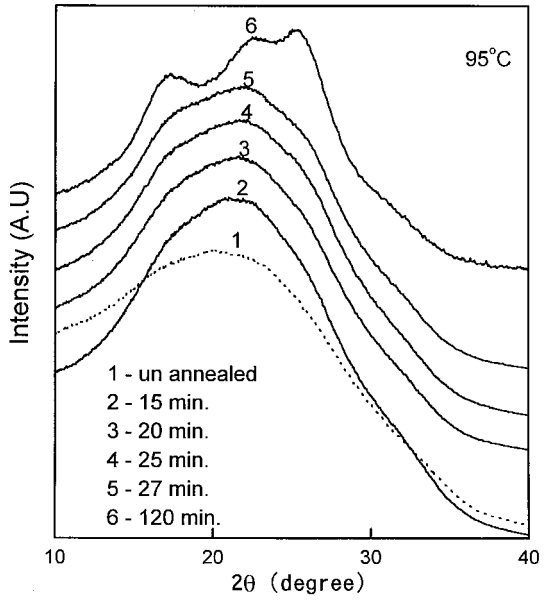

Fig. 2. WAXD intensity profiles at different time intervals for the samples with draw ratio (DR) = 2during isothermal crystallization at 95°C.

of crystallization were investigated by FTIR, whereas the process of crystal formation was investigated by WAXD. SAXS studies also were used to investigate the development of density fluctuation. Emphasis was given to understanding of the structural organizations before the crystallization.

2. Experimental

2.1. Materials and sample preparation

The pellets of PET with intrinsic viscosity, $\eta_{inh} = 0.62$ were obtained from scientific polymer products Co. Ltd. Amorphous PET films were prepared by hot pressing the pellets at 295°C using a compression molder and quickly quenching the film into ice water. Oriented samples were prepared by the following method. The quenched amorphous samples were placed between two polypropylene sheets of 1 mm thickness and were drawn using rolling machine at 30°C to a draw ratio of 2. The rolled PET film was essentially amorphous as indicated by X-ray diffraction patterns and the density measurements (density = 1.335 g/cm^3). As the PET films were crystallized by stretching them to a draw ratio higher than 2.5, only sample of draw ratio 2 was used for the studies.

2.2. FTIR studies

Thin oriented films of PET were mounted on a hot stage, Mettler FP82HT, and secured firmly using tapes to prevent any thermal shrinkage. The sample was then quickly heated to the crystallization temperature and the polarized FTIR spectra were recorded with time. The polarized FTIR spectra were recorded with a Bio-rad FTS 60A-686 FTIR spectrophotometer equipped with a wire-grid polarizer. Each spectrum was taken for 15 s at an interval of 2 or 5 min.

2.3. Wide-angle X-ray diffraction studies

Film samples were mounted on a hot stage as was done in the FTIR studies. Samples were then heated to the crystallization temperature and WAXD patterns were obtained with time on the imaging plates (IP) using a monochromatized CuK_α radiation of wavelength $\lambda = 0.1542$ nm (40 kV, 100 mA) generated by a Rotaflex RU-300 X-ray diffractometer (Rigaku Co. Ltd.). Digitized data were then read from the IP using imaging plate reader. Using IP, very small change in WAXD patterns could be obtained with an exposure time as short as 1 min.

2.4. Small angle X-ray scattering studies

Samples were isothermally heat-treated at 93°C for various time periods and quenched into liquid nitrogen immediately after the crystallization time was completed to ensure that the structure developed in the annealing process is preserved. SAXS studies were carried out using

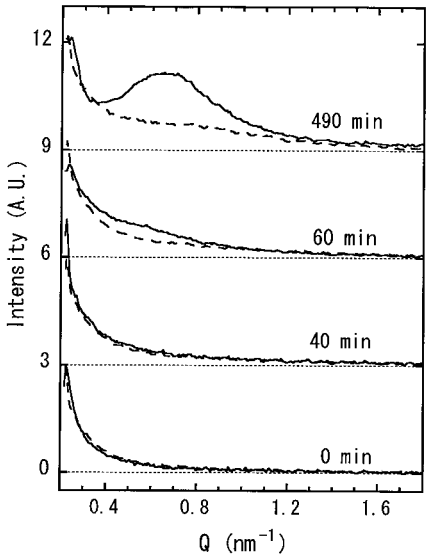

Fig. 3. Meridional and equatorial SAXS profiles of the oriented PET film (DR = 2) heat-treated at 93°C for various time periods. Q is $(4\pi/\lambda)\sin\theta$: Meridional profile (—); equatorial profile (– – –).

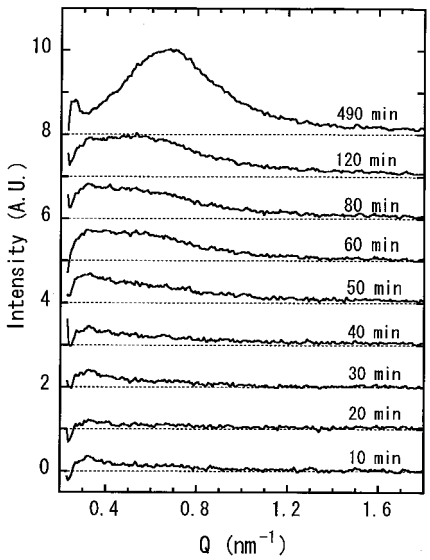

Fig. 4. Difference meridional SAXS profiles of the oriented PET film (DR = 2) heat-treated at 93°C for various time periods. The difference profile was obtained by subtracting the meridional profile before heat-treatment from that of heat-treated samples.

a CuK_α radiation generated by a Rigaku Ultrax 8000 X-ray diffractometer, and a point-focusing SAXS camera. The camera length used was 290 mm and the images were recorded using IP with an exposure time of 2 h. Small changes in the SAXS patterns could be accurately obtained using the IP.

3. Result

3.1. Wide-angle X-ray diffraction studies

Figs. 1 and 2 show the WAXD intensity profiles obtained for the samples with draw ratio (DR) = 2 during the isothermal crystallization at temperatures of 93 and 95°C, respectively, at different time intervals. The appearance of the 010, 110, and 100 reflections is clearly evident in the WAXD intensity profiles. It is noted that the WAXD data do not show any indication of crystalline reflections up to a time interval of 50 min for the isothermal crystallization at 93°C. The crystallization starts at 25 min for isothermal crystallization at 95°C. The crystallization rate is increased with the rise in crystallization temperature. The WAXD intensity due to the amorphous phase gradually increases with time before the crystalline reflection appears. This result shows that the ordering of the non-crystalline chains proceeds prior to the crystallization. The crystal reflections become sharper and are intensified with time after the start of the crystallization (50 min for 93°C and 25 min for 95°C). The degree of crystallinity and the crystalline order gradually increases with time in these time periods.

3.2. Small angle X-ray scattering studies

Fig. 3 shows the meridional and equatorial SAXS profiles for the oriented sample, during the heat-treatment at 93°C for various time periods. The SAXS intensity was normalized by the sample thickness after air scattering was subtracted from the observed SAXS profile. Fig. 4 shows the difference meridional SAXS profiles obtained by subtracting the SAXS profile before heat-treatment from the SAXS profiles of heat-treated samples. Fig. 5 shows the difference of the meridional SAXS profiles from the equatorial profile as a function of heat-treatment time. The SAXS intensity increases with increasing heat-treatment time both in the equatorial and meridional profiles. The crystal reflection appears on the WAXD profile of the sample heat-treated for the period longer than 60 min. The SAXS intensity begins to increase with time in the induction period of crystallization. The difference SAXS profile in Fig. 4 shows that a peak appears around $Q =$ 0.3–0.4 nm^{-1} in the early stage (10–30 min) of reorganization of oriented PET [1,2]. Imai et al. also reported that the SAXS intensity starts to increase at $Q = 0.2$–0.4 nm^{-1} in the induction period of the isothermal crystallization of isotropic PET [1,2]. The peak at $Q = 0.3$–0.4 nm^{-1} in the difference profile of Fig. 4 is considered to correspond to the low angle SAXS observed in the induction period of crystallization of isotropic PET. Fig. 5 shows that the intensity of the equatorial profile is slightly higher than the meridional profile in the as-rolled film (0 min), in the low angle range ($Q = 0.3$–0.5 nm^{-1}). This tendency remains in the samples heat-treated for 10–20 min, and the SAXS profile is nearly isotropic before 40 min, indicating that the density fluctuation grown in the early stage of the structural organization (<30 min) is nearly isotropic. On the other hand, the intensity of the meridional profile exceeds that of the equatorial profile after 40 min. A positive peak appears at

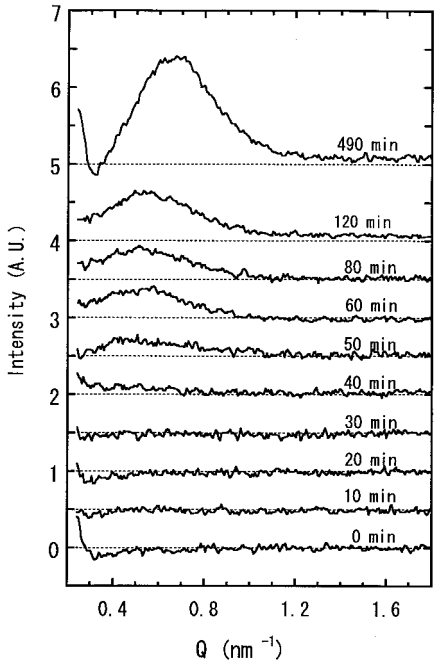

Fig. 5. Difference SAXS profile of the oriented PET film (DR = 2) heat-treated at 93°C for various time periods. The difference profile was obtained by subtracting the equatorial SAXS profile from the meridional SAXS profile.

$Q = 0.4$–$0.5\ \mathrm{nm}^{-1}$ in the difference profile of Fig. 5 at 50 min. The peak increases in intensity and gradually shifts to the larger value of Q. The isotropic density fluctuation formed in the early stage is organized into the oriented density fluctuation parallel to the meridian. The long period of the oriented density fluctuation is 14 nm ($Q = 0.45\ \mathrm{nm}^{-1}$) at 50 min, and gradually decreases with increasing the heat-treatment time resulting in the formation of the regular long period with a period of 10 nm ($Q = 0.65\ \mathrm{nm}^{-1}$)

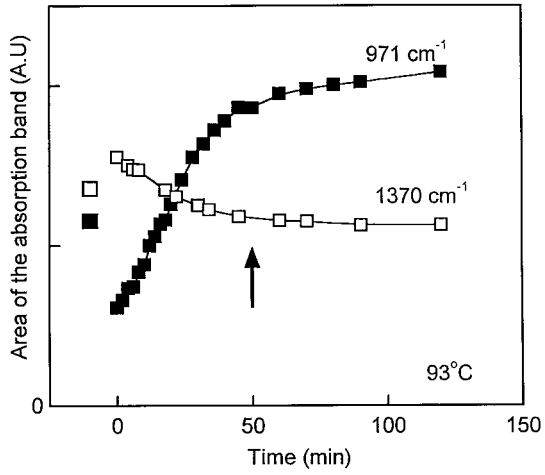

Fig. 6. Areas of the 971 and 1370 cm^{-1} bands as a function of time during isothermal crystallization at 93°C. The arrow represents the time when the crystalline reflections appear in the WAXD diagram.

in the sample heat-treated for 490 min. The time-resolved SAXS studies have been carried out to investigate the mechanism of primary nucleation in the crystallization of isotactic polypropylene during melt extrusion [16]. The oriented SAXS pattern develops parallel to the extrusion direction before crystalline peaks appear in the WAXD, indicating that the long-range order develops prior to crystallization of polypropylene. The SAXS peak was shown to shift to the higher angle (the larger values of Q) with the onset of crystal growth [16]. The time-resolved SAXS studies during the isothermal crystallization of polyethylene showed that the long-range order with a period of 80 nm develops at the initial stage of crystallization before the development of the regular long period with densely packed lamellae [17]. The SAXS results of the present studies are considered to be similar to the cases of these works [16,17].

3.3. FTIR studies

To understand the structure formation prior to the crystal formation, we analyzed the FTIR data. The detailed analysis of the absorption bands in PET has been reported [18–21]. In this study the two bands at 971 and 1370 cm^{-1} were used for the analysis, as these bands are relatively isolated from other bands. The 971 cm^{-1} band has been assigned to the C–O stretching vibration of the *trans* units in the ethylene glycol linkage and the contribution comes from both crystalline and amorphous phases. The band at 1370 cm^{-1} is assigned to the CH_2 wagging mode of the *gauche* conformer.

The absorption intensities were obtained by integrating the area under the absorption bands. The dichroic ratio, D and the area intensity, A, were obtained from the absorption intensities, A_{para} and A_{perp}, for the parallel and perpendicular polarizations, respectively, as a function of crystallization time.

$$D = A_{\mathrm{para}}/A_{\mathrm{perp}} \tag{1}$$

$$A = (A_{\mathrm{para}} + 2A_{\mathrm{perp}})/3 \tag{2}$$

Fig. 6 shows the areas of the 971 and 1370 cm^{-1} bands as a function of time during isothermal crystallization at 93°C. The absorption intensities are normalized by the thickness of samples. The structural organization in the induction period consists of the two processes. The absorption intensity of the 971 cm^{-1} band decreases and that of the 1370 cm^{-1} band increases, when heated from room temperature to the crystallization temperature. The *trans* conformation is transformed into the *gauche* conformation at the initial stage of the isothermal process. This may be due to the thermodynamic relaxation occurring in the beginning when the samples are heated above its T_g, which is close to 70°C. The area of the *trans* band starts to increase and that of the *gauche* band starts to decrease at 10 min from the start of the isothermal process. The conformational transition from *gauche* to *trans* gradually proceeds in the second

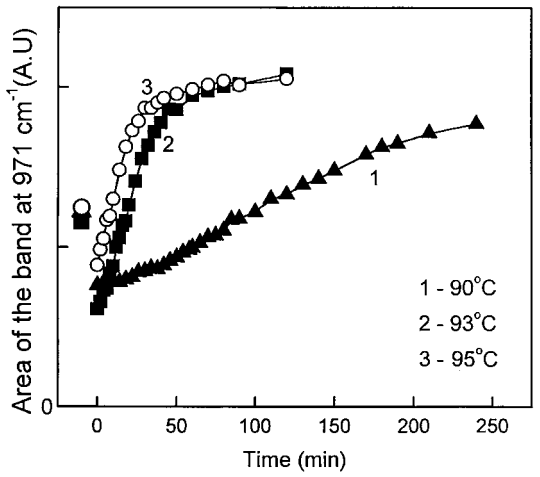

Fig. 7. Areas of the 971 cm^{-1} band at the three crystallization temperatures studied viz. 93, 95, and 90°C as a function of time.

stage (10–50 min), and absorption intensities of the two bands level off to constant values simultaneously at 60 min.

Fig. 7 shows the area under the band at 971 cm^{-1} at the three crystallization temperatures studied viz. 93, 95, and 90°C as a function of time. The absorption intensity was normalized by the thickness of samples. The absorption intensity of the *trans* band decreases at the initial stage and gradually increases to a constant value in the second stage. The effect of temperature on the reorganization kinetics is evident in the in situ FTIR results. The intensity of the sample crystallized at 95°C increases to a constant value rapidly as compared to the other two temperatures. The increase in absorption intensity levels off to a constant value at 50 min for 93°C and 25 min for 95°C, almost simultaneously with the appearance of crystalline reflections in the WAXD profile. On the other hand, saturation in the increase in the absorption intensity was not observed for the isothermal process at 90°C. The sample heat-treated at 90°C did not show any crystalline reflections even up to a time period of 4 h.

To investigate the changes in the orientation order during the crystallization, we have examined the change of dichroic ratio of the 971 cm^{-1} band for all the crystallization temperatures studied. The degree of orientation increases with increasing the value of dichroic ratio because the 971 cm^{-1} band is the parallel-polarized band. Fig. 8 shows the dichroic ratio as a function of time at the crystallization temperatures of 93 and 95°C. The orientation process consists of two stages as was found for the conformational transition. The dichroic ratio of the 971 cm^{-1} band decreases to a value of 1.1–1.2, when heated from room temperature to the crystallization temperature. The orientation was randomized to nearly isotropic state in the first stage of the reorganization. The dichroic ratio starts to increase again at 10 min from the start of the isothermal process for the isothermal crystallization at 93°C, and markedly increases with time in the second stage of the induction period for all the crystallization temperatures. The orientation process of molecular chains is suppressed after the crystal reflection appears in the WAXD intensity profiles, at 50 min for 93°C and at 25 min for 95°C.

Fig. 9 shows the dichroic ratio as a function of time for the isothermal process at 90°C. The dichroic ratio showed gradual increase with time after the initial decrease and did not level off to constant value even up to a time period of 4 h. The WAXD studies do not show any indication of crystalline reflections even after a crystallization time of 4 h in this case.

Fig. 10 shows the dichroic ratio of the 1370 cm^{-1} band of the sample crystallized at 93°C. The degree of orientation of the *gauche* conformer steeply decreases in the initial stage of the isothermal process, and the perpendicular orientation

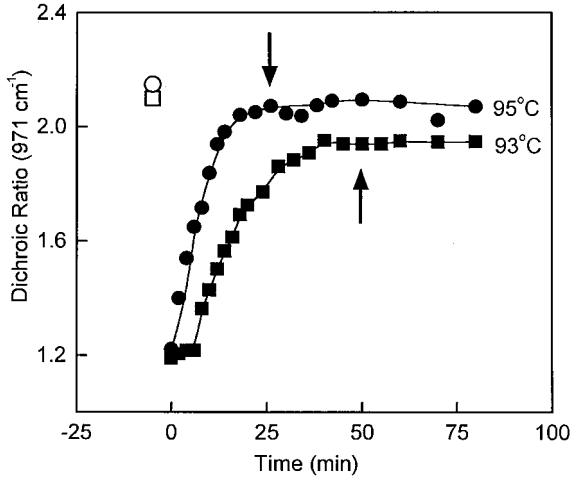

Fig. 8. Dichroic ratio of the 971 cm^{-1} band as a function of time during isothermal crystallization at 93 and 95°C. The arrow represents the time when the crystalline reflections appear in the WAXD diagram: (○, □) As-rolled film; (●, ■) During isothermal crystallization.

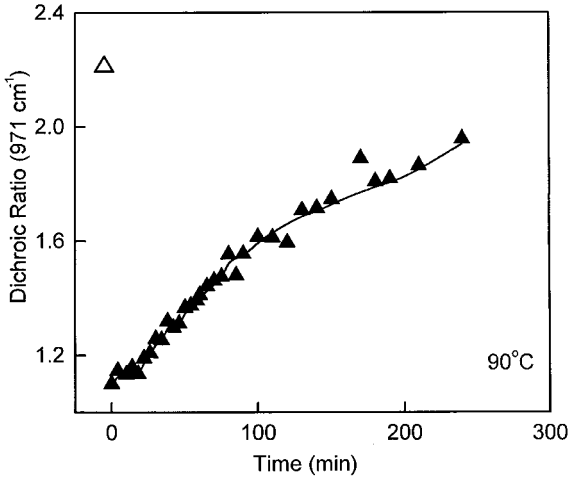

Fig. 9. Dichroic ratio of the 971 cm^{-1} band as a function of time during isothermal crystallization at 90°C: (△) As-rolled film; (▲) During isothermal crystallization.

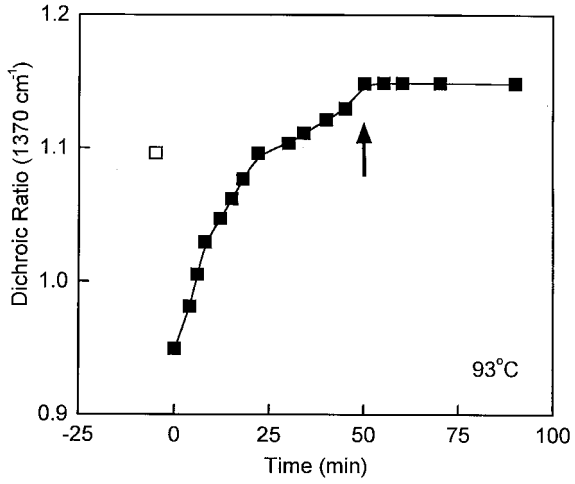

Fig. 10. Dichroic ratio of the 1370 cm^{-1} band as a function of time during isothermal crystallization at 93°C. The arrow represents the time when the crystalline reflections appear in the WAXD diagram: (□) As-rolled film; (■) During isothermal crystallization.

is developed in the very beginning. The dichroic ratio (degree of orientation) showed a marked increase in the second stage as in the case of the dichroic ratio of the 971 cm^{-1} band. The orientation behavior of the gauche conformation is however different from that of the *trans* conformer. The dichroic ratio of the initial state of the *trans* band is as large as that of the last state, while the dichroic ratio of the *gauche* band in the final state exceeds that of the initial state. The oriented morphology is developed by the cold rolling, but the molecular motion is restricted at the rolling temperature (30°C). The rolling stress induces the orientation and conformation change simultaneously in the molecular chains, while some unstressed chains with *gauche* conformation remain nearly isotropic in the case of the rolling below T_g. As temperature rises above T_g, however, the molecular motion facilitates the reorganization of the whole oriented structure. The degree of orientation of the *gauche* conformation increases simultaneously with the orientation development of the *trans* conformers. Finally the degree of orientation of the *gauche* conformer exceeds the amount of the initial state during the isothermal crystallization.

4. Discussion

4.1. Structure organization during isothermal crystallization

The structural organization during the isothermal crystallization of oriented PET consists of three stages. The conformational transition from *gauche* to *trans* takes place, and the molecular orientation is relaxed into the nearly isotropic level in the first stage of the isothermal crystallization (0–8 min at 93°C). The second stage is the self-organization process of the oriented amorphous structure, in which the degree of orientation gradually increases with time and the *gauche* conformation is transformed into the *trans* conformation (10–50 min at 93°C). The SAXS studies showed that the isotropic density fluctuation develops in the early stage of reorganization, but the density fluctuation begins to orient to the stress direction in the latter half of the second stage. The crystallization begins in the third stage (after 50 min at 93°C). The crystallinity and the crystalline order increase with time, but the degree of orientation and the *trans* content are kept constant. The long period of the density fluctuation decreases in the third stage, resulting in the formation of the regular long period of lamellar stacks.

Blundell et al. studied the orientation and the crystallization process during fast drawing of PET using synchrotron radiation X-ray studies [12–15]. They discussed the phenomena on the basis of the theory of an enclosing tube by Doi and Edward [22] and the concept of reputation by de Gennes [23]. The fastest relaxation process is the molecular motion between entanglements, which can be regarded as a fixed cross-link on a time scale of this relaxation process [15]. The second process with intermediate relaxation time involves a retraction of chains within the deformed tube in order to recover their equilibrium curvilinear length. The third process with longer relaxation time is the reptation of chains out of their original tubes to form new tubes. They found that the onset of crystallization is delayed until the end of drawing when the draw rate is faster than the chain retraction process. This is because the chains do not have the freedom and the mobility to organize into crystals during deformation as long as the deformation rate is fast compared with the chain retraction processes [15]. But when the draw rate becomes comparable to the rate of chain retraction process, the crystallization starts during the draw process [15].

The reorganization during the isothermal crystallization of oriented PET can be explained in terms of the tube model. The thermodynamic relaxation occurs in the first stage of the reorganization, when the samples are heated above its T_g. In the oriented samples, the molecular chains are oriented in the global sense whereas the local segments may be at a lower degree of orientation. The initial relaxation process is due to the relaxation of the local segments, originating from the molecular motion within the deformed tube. The significant ordering process occurs in the oriented amorphous state prior to the crystallization in the second stage, which involves the reptation of chains out of their original tubes to form new tubes. The global configurations of molecular chains are reorganized into a highly oriented one and the local segments undergo the orientation process to the axis of the oriented tube.

The results by Blundell et al. suggested that the strain-induced crystallization was closely related to the chain retraction process with intermediate relaxation time [15]. In their experiment, the degree of orientation is high enough that oriented molecular chains are crystallized in a short time

only by changing their equilibrium positions within the tube. On the other hand, the rate of crystallization is much slower in our experiment than in their experiment. The draw ratio of the starting sample is as low as 2 in our case, and the degree of orientation is not so high that the molecular chains cannot be organized into crystal by the chain retraction process. The molecular chains are relaxed by the molecular motion within the tube, instead of being crystallized when the draw ratio is below 2.0. As time goes by, however, the relaxed molecular chains are reorganized into highly oriented state by the chain reptation process with longer relaxation time.

The effect of temperature on the rate of structural organization is evident here. The induction period becomes shorter with the rise in crystallization temperature. This is because the molecular motion facilitates the reorganization in the induction period at high temperature. The degree of orientation is higher or comparable in the heat-treated sample than in the as-drawn sample, suggesting that the heat-treatment of oriented amorphous materials under constraint provides a useful method for processing the highly oriented materials.

4.2. Comparison of the crystallization behavior between oriented PET and isotropic PET

The reorganization process prior to the crystallization of the oriented PET has something common with the crystallization of the isotropic PET. Imai et al. [1–4] suggested that in the case of isotropic PET some rod-like segments of chains started to orient parallel to one another in the induction period of crystallization. In the present case, the samples used have some degree of orientation. The increase and subsequent leveling off of dichroic ratio prior to the appearance of crystalline reflections indicate that parallel ordering of the polymer chains takes place before the crystallization in the oriented materials also. In the case of isotropic PET, the orientation fluctuation of polymer segments causes the density fluctuation in the early stage of the induction period [3]. The evolution of the density fluctuation is in accordance with the theory of spinodal decomposition [2]. In the case of oriented PET, the degree of orientation increases with time due to the internal stress. It is considered that the mutual alignment of molecular chains is induced by the stress in the case of oriented crystallization, and that the degree of orientation plays an essential role in the formation of density fluctuation. In this work, the tube model was used to explain the orientation process during the crystallization of oriented PET. The analogous argument might be applicable to the growing process of orientation fluctuation during the crystallization of isotropic PET.

Figs. 6 and 7 show that the area intensity of the *trans* band increases very little after the crystallization starts. On the other hand, Matsuba et al. observed that the crystalline conformations of isotactic and syndiotactic polystyrenes begin to increase before crystal nucleation, and the increase of the crystalline conformation is more marked in the period of the crystal growth than in the induction period [24,25]. The difference is considered to arise from the orientation effects. The absorption intensity of the 971 cm^{-1} band, which is assigned to the *trans* conformation both in the amorphous and crystal phases [26], is much lower in the isotropic amorphous sample than in the oriented amorphous film, suggesting that the molecular chains in the quenched film favor the *gauche* conformation and that the conformation transition from *gauche* to *trans* is induced by the orientation of molecular chains even in the amorphous state. The *trans* conformers in the amorphous phase tend to crystallize in the isotropic films, whereas the *trans* conformers are stabilized by the internal stress even in the amorphous phase in the case of the oriented films. The rate of crystallization is much faster in the oriented film than in the isotropic film, suggesting that the crystallization is induced by the high degree of orientation. The *trans* conformers stabilized by the oriented structure remain in the amorphous phase until the degree of orientation increases to a certain level that is required for the crystallization. We have also carried out the isothermal crystallization of oriented isotactic polystyrene films [27]. The degree of orientation increases with time mostly before the crystalline reflections appear in the WAXD profiles, as was found in the case of PET.

5. Conclusions

Oriented films of PET were prepared by rolling method and the crystallization behavior of the oriented PET was investigated using in situ FTIR, WAXD, and SAXS studies. Measuring the change in dichroic ratio using polarized in situ FTIR monitored the change in orientation with time. The development of crystalline structure was investigated by in situ WAXD studies. The structural organization in the isothermal crystallization of oriented PET consists of three stages. The first stage involves the thermodynamic relaxation, when the samples are heated above its T_g. The conformational transition from *gauche* to *trans* takes place, and the molecular orientation is relaxed into the nearly isotropic level in the first stage of the isothermal crystallization. The second stage is the self-organization process of the oriented amorphous structure, in which the degree of orientation markedly increases with time and the *gauche* conformation is transformed into the *trans* conformation. The SAXS studies showed that the isotropic density fluctuation develops in the early stage of reorganization, but the density fluctuation begins to orient to the stress direction in the latter half of the second stage. The third stage is the crystallization of oriented molecular chains into the crystal lattice. The degree of orientation and the *trans* contents become constant in this stage. The long period of the density fluctuation decreases in the third stage, resulting in the formation of the regular long period of lamellar stacks. These observations give evidence to the concept that ordering of the polymer chains occurs during the induction period of crystallization. The possible mechanism was discussed

on the basis of the tube model. The initial relaxation process was interpreted to originate from the molecular motion within the tube, whereas the second reorganization process is due to the chain reptation motion in the oriented structure.

Acknowledgements

The authors wish to thank Dr Yoshikazu Tanabe of National Institute of Materials and Chemical Research for hearty encouragement and valuable suggestions.

References

[1] Imai M, Mori K, Mizukami T, Kaji K, Kanaya T. Polymer 1992;33:4451.
[2] Imai M, Mori K, Mizukami T, Kaji K, Kanaya T. Polymer 1992;33:4457.
[3] Imai M, Kaji K, Kanaya T. Macromolecules 1994;27:7103.
[4] Imai M, Kaji K, Kanaya T. Phys Rev Lett 1993;71:4162.
[5] Ezquerra TA, Lopez-Cabarcos E, Hsiao BS, Balta-Calleja FJ. Phys Rev E 1996;54:1996.
[6] Kimura T, Ezure H, Tanaka S, Ito E. J Polym Sci, Polym Phys 1998;36:1227.
[7] Matsuba G, Kaji K, Nishida K, Kanaya T, Imai M. Polym J 1999;31:722.
[8] Kimura F, Kimura T, Sugisaki A, Komatsu M, Sata H, Ito E. J Polym Sci, Polym Phys 1998;35:2747.
[9] Smith FS, Steward RD. Polymer 1974;15:283.
[10] Alfonso GC, Verdona MP, Wasiak A. Polymer 1978;19:711.
[11] Asano T, Balta Calleja FJ, Flores A, Tanigaki M, Mina MF, Sawatari C, Itagaki H, Takahashi H, Hatta I. Polymer 1999;40:6475.
[12] Blundell DJ, MacKerron DH, Fuller W, Mahendrasingam A, Martin C, Oldman RJ, Rule RJ, Riekel C. Polymer 1996;37:3303.
[13] Mahendrasingam A, Martin C, Fuller W, Blundell DJ, Oldman RJ, MacKerron DH, Harvie JL, Riekel C. Polymer 1999;41:1217.
[14] Mahendrasingam A, Martin C, Fuller W, Blundell DJ, Oldman RJ, MacKerron DH, Harvie JL, Riekel C, Engstrom P. Polymer 1999;41:1217.
[15] Blundell DJ, Oldman RJ, Fuller W, Mahendrasingam A, Martin C, MacKerron DH, Harvie JL, Riekel C. Polym Bull 1999;42:357.
[16] Terrill NJ, Fairclough PA, Towns-Andrews E, Komanschek BU, Young RJ, Ryan AJ. Polymer 1998;39:2381.
[17] Sasaki S, Tashiro K, Kobayashi M, Izumi Y, Kobayashi K. Polymer 1999;40:7125.
[18] Miyake A. J Polym Sci 1959;19:485.
[19] Boerio FJ, Bahl SK, McGraw GE. J Polym Sci, Polym Phys Ed 1976;14:102.
[20] Schmidt PG. J Polym Sci A 1963;1:1271.
[21] Liang CY, Krim S. J Mol Spectrosc 1959;3:554.
[22] Doi M, Edward SF. The theory of polymer dynamics. Oxford: Clarendon, 1986.
[23] de Gennes P-G. J Chem Phys 1971;55:572.
[24] Matsuba G, Kaji K, Nishida K, Kanaya T, Imai M. Polym J 1999;31:722.
[25] Matsuba G, Kaji K, Nishida K, Kanaya T, Imai M. Macromolecules 1999;32:8932.
[26] Ito M, Perreira JRC, Hsu SL, Porter RS. J Polym Sci, Polym Phys 1983;21:389.
[27] Radhakrishnan J, Kaito A. Polym Prepr Jpn 2000;49(3):413.